ACS APPLIED MATERIALS & INTERFACES

Research Article

www.acsami.org

Solid-Phase Covalent Immobilization of Upconverting Nanoparticles for Biosensing by Luminescence Resonance Energy Transfer

Samer Doughan, Yi Han, Uvaraj Uddayasankar, and Ulrich J. Krull*

Chemical Sensors Group, Department of Chemical and Physical Sciences, University of Toronto Mississauga, 3359 Mississauga Road, Mississauga, Ontario L5L 1C6, Canada

Supporting Information

ABSTRACT: Monodisperse water-soluble upconverting nanoparticles (UCNPs) were immobilized onto modified glass substrates for development of biosensing surfaces that operated using luminescence resonance energy transfer (LRET). Amine modified UCNPs were prepared from oleic acid capped UCNPs by ligand exchange using *o*-phosphorylethanolamine (PEA). PEA-UCNPs were covalently immobilized on aldehyde functionalized coverslips. Environmental scanning electron microscopy (ESEM) images indicated a homogeneous distribution of UCNPs on surfaces with a high immobilization density of approximately 1.3×10^{11} UCNP cm^{-2}. This is the first account of covalent immobilization of UCNPs for bioassay and biosensor development where the density is on par with the high immobilization densities reported for other types of nanoparticles. The functionality and stability of the immobilized NPs were demonstrated by examining an LRET-based bioassay. The well-known sandwich assay for the detection of thrombin was selected as a model in which UCNPs were used as donors and quantum dots (QDs) as acceptors. The closely packed UCNPs on the glass surface showed a 2.5-fold enhancement in assay sensitivity compared to less-densely packed surfaces. In addition, a 1.5-fold enhancement in energy transfer efficiency was shown for solid-phase compared to solution-phase LRET.

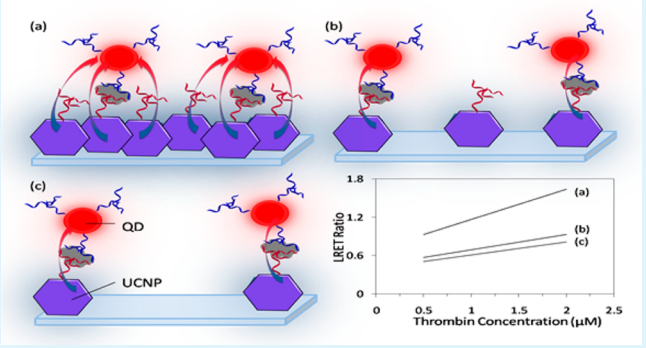

KEYWORDS: *upconverting nanoparticles, quantum dots, luminescence resonance energy transfer, solid-phase assay, biosensor*

INTRODUCTION

Over the past decade, UCNPs have attracted much attention in the field of bioanalysis. Various unique optical properties and relative compatibility with biological systems suggest that UCNPs may be useful in both *in vivo* and *in vitro* applications.[1−3] UCNPs are lanthanide doped inorganic crystals that are excited by near-infrared (NIR) or infrared (IR) radiation, with subsequent emissions in the UV, visible, and near IR regions of the spectrum. Upconversion (UC) is based on the sequential absorption of photons, and the various processes that lead to photon UC have been thoroughly reviewed.[3,4] Compared to traditional fluorescent labels, UCNPs have the potential to offer improved signal-to-noise since excitation in the NIR region ameliorates background signal associated with optical scatter and autofluorescence from samples of biological origin.[5] In addition, UCNPs exhibit narrow and well-defined emission peaks, offering an opportunity to simultaneously operate at a variety of wavelengths for multiplexing, either as passive labels or as luminescence resonance energy transfer (LRET) donors. Various examples of bioassays using UCNPs for the detection of proteins have been reported. Examples include UCNPs as labels for cell surface proteins,[6,7] as passive labels for protein detection in lateral flow devices,[8−11] and as LRET donors in solution with acceptors such as fluorescent proteins,[12] organic dyes,[13] gold nanoparticles (AuNPs),[14] and carbon nanoparticles (CNPs).[15,16] Bioassays for the detection of DNA,[17−20] metabolites,[21−23] and metal ions[24−27] have been reported.

Recently, LRET bioassays based on adsorbed UCNPs on paper substrates have been reported for the detection of matrix metalloproteinase-2 (MMP-2)[28] and single-stranded DNA.[29] The use of nanoparticles (NPs) at interfaces offers several advantages over solution phase assays. Immobilization of NPs avoids problems associated with aggregation of particles in solution and allows for facile layer-by-layer decoration without the need for time-consuming and tedious purification steps. More specific to LRET assays, luminescent NPs are expected to offer improved LRET efficiencies at interfaces as a result of high densities of donor and acceptor at the surface, where there is potential for a single acceptor to interact with multiple donors.[30−32] Such intrinsic amplification would assist to offset the limited LRET efficiencies for UCNPs when used as donors, as these efficiencies are typically much lower than 50%. Processes that amplify emission intensity would tend to

Received: May 29, 2014
Accepted: July 21, 2014
Published: July 21, 2014

dx.doi.org/10.1021/am503391m | ACS Appl. Mater. Interfaces 2014, 6, 14061−14068

improve sensitivity and detection limits of bioassays.[13] Strategies to improve UCNP assays that are based on LRET have included surface decoration of UCNPs,[23] optimization of properties of the LRET acceptor,[15,33] and adjustment of the spatial distance dependency by appropriate assay design.[13,15] The work presented herein investigates a different approach to improve bioassays that use UCNPs for LRET.

The LRET-based solid-phase bioassays that have been reported in the literature make use of adsorbed UCNPs on surfaces.[29] Such systems are susceptible to desorption of UCNPs, suggesting a general instability of the transduction system and also the potential to bypass the signal enhancement opportunity that comes from immobilization at high density. Covalent immobilization of UCNPs at high density would offer a sensitive transduction platform with potential for washing, regeneration, and a wider range of stringency control to influence biomolecule affinity and selectivity. Numerous examples of NP immobilization on glass substrates have been reported for bioassays. Petryayeva et al. reported multidentate imidazole surface ligands for the immobilization of QDs and AuNPs for the transduction of nucleic acid hybridization and enzyme activity.[34] Nath et al. demonstrated a self-assembled monolayer of colloidal gold on amine modified glass coverslips for the detection of streptavidin.[35] Tavares et al. immobilized streptavidin coated QDs on biotinylated coverslips with the intention of determining the presence of oligonucleotides within microfluidic channels.[30] Typically, immobilization of NPs on solid interfaces for transduction by fluorescence makes use of covalent linkages or multidentate surface ligand association, and such immobilization methods for QDs, CNPs, and AuNPs are well established,[32] but this is not the case for UCNPs.

Herein we describe a facile method for generating water-soluble core/shell UCNPs from oleic acid capped UCNPs by ligand exchange and explore the covalent immobilization of the amine decorated UCNPs on aldehyde modified glass substrates. The stability and utility of the immobilized UCNPs is demonstrated by means of a model LRET-based solid-phase bioassay showing an enhancement in assay performance for high immobilization densities of monolayers of UCNPs.

EXPERIMENTAL SECTION

For detailed experimental procedures and information on materials and instruments used, the reader is referred to Figure 1, Table 1, and Supporting Information.

Synthesis of Core/Shell UCNPs. Core $NaYF_4$: 0.5% Tm^{3+}, 30% Yb^{3+} UCNPs were synthesized according to the literature with minor changes.[36] In brief, 0.4560, 0.2533, and 0.0042 g of $Y(CH_3CO_2)_3{\cdot}xH_2O$, $Yb(CH_3CO_2)_3{\cdot}4H_2O$, and $Tm(CH_3CO_2)_3{\cdot}xH_2O$ were stirred under vacuum in 30 mL octadecene and 12 mL oleic acid (OA) at 115 °C for 30 min. The temperature was then lowered to 50 °C with the mixture capped under argon. A 20 mL methanol solution containing 0.20 g NaOH and 0.2965 g NH_4F was added and the reaction was stirred for 30 min, after which the temperature was raised to 75 °C to evaporate the methanol. The solution was then rapidly heated to 300 °C and maintained at that temperature for 75 min. The solution was allowed to cool to room temperature and the product was precipitated using ethanol and centrifugation at 4500 rpm. Core UCNPs were then washed in hexanes and recaptured with ethanol and centrifugation. The washed cores were stored in hexanes at 4 °C.

Processing of the core UCNPs continued and $NaYF_4$: 0.5% Tm^{3+}, 30% Yb^{3+}/β-$NaYF_4$ core/shell UCNPs were prepared by stirring 0.5741 g $Y(CH_3CO_2)_3{\cdot}xH_2O$ under vacuum in 30 mL octadecene and 12 mL OA at 115 °C for 30 min. The temperature was lowered to 80 °C under argon and core UCNPs in hexanes were added. The reaction was maintained at 80 °C until all hexanes were removed. The reaction was treated with a 20 mL methanol solution containing 0.14 g NaOH and 0.2590 g NH_4F and the reaction was stirred for 30 min, after which the temperature was raised to 75 °C to evaporate the methanol. The solution was then rapidly heated to 300 °C and maintained at that temperature for 75 min. The product was precipitated using ethanol and centrifugation at 4500 rpm. The precipitate was redissolved in hexanes and precipitated with ethanol and collected by centrifugation for a total of three times, and the core/shell UCNPs were then stored in hexanes.

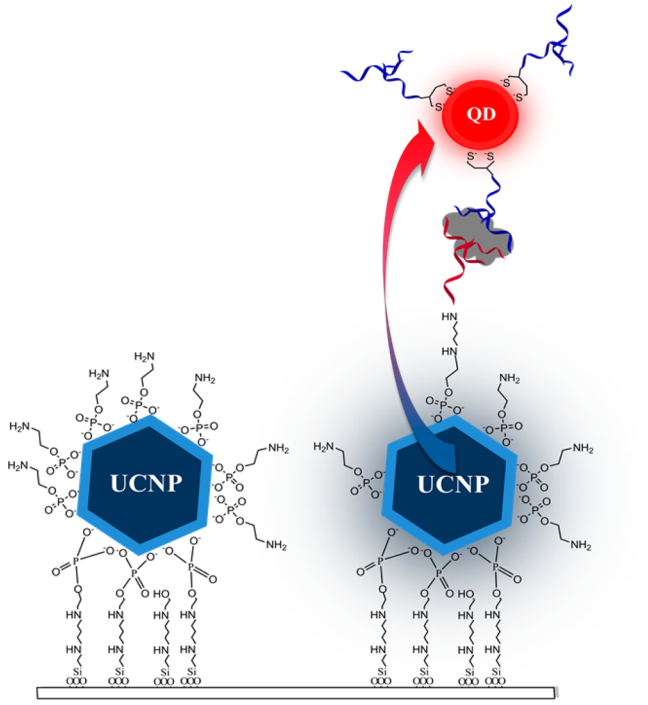

Figure 1. Schematic showing immobilization of PEA-UCNP on aldehyde functionalized coverslip and use in the detection of thrombin (gray) using thrombin-specific aptamer-1 (red) and aptamer-2 (blue).

Table 1. Aptamer Sequences Used for Thrombin Detection

	sequence	K_d
Aptamer-1	5′-Amine C6-AGT CCG TGG TAG GGC AGG TTG GGG TGA CT-3′	0.5 nM[43]
Aptamer-2	5′-DTPA-GGT TGG TGT GGT TGG-3′	25−200 nM[44]

Preparation of Water-Soluble UCNPs. Hydrophilic UCNPs were prepared based on a literature protocol with some modifications.[37] In a glass vial, 400 mg of *o*-phosphorylethanolamine (PEA), 6 mL of absolute ethanol, and 1 mL of tetramethylammonium hydroxide (TMAH) were added to 2 mL of 100 mg OA acid capped UCNPs in hexanes. The solution was allowed to stir overnight at 70 °C.

PEA-UCNPs were recovered by centrifugation at 3500 rpm. The UCNPs were washed three times using ethanol via sonication and recovered by adding hexanes followed by centrifugation at 4500 rpm. The UCNPs were then suspended in 10 mL of purified water (Milli-Q) and sonicated for 10 min before passage through a 0.2 μm poly(ether sulfone) (PES) syringe filter to remove any large aggregates. The solution was stored in purified water at 4 °C.

Surface Modification of Coverslips. Glass coverslips were processed using the RCA (Radio Corporation of America) cleaning procedure.[38] This involved the use of a NH_4OH wash followed by an HCl wash, both in the presence of hydrogen peroxide in a 5:1:1 ratio of water (acid or base) hydrogen peroxide. This process removed organic and inorganic contaminants and generated silanol groups on the glass surface. These silanols were then coupled to 3-amino-

propyltrimethoxysilane (APTMS) to modify the surface with amine functionality. The reaction proceeded by adding 15 mL of APTMS and 1 mL of *N*,*N*-diisopropylethylamine (DIPEA) in 220 mL of toluene for concurrent treatment of 32 coverslips. The reaction was allowed to reflux for 6 h at 80 °C under argon. The coverslips were sequentially washed using methanol, dichloromethane, and ethyl ether and were then stored in a desiccator.

Aldehyde functionalized coverslips were obtained as reported in the literature.[39] In brief, 8 amine modified coverslips were placed in a solution of 24 mL glutaraldehyde (25% in H_2O) with 36 mL 1×PBS (phosphate buffered saline) (pH 7.4) and 0.1 g of sodium cyanoborohydride. The solution was allowed to shake for 2 h in the dark. The coverslips were then washed with purified water (Milli-Q) and stored in a desiccator in the dark. All slides were characterized using X-ray photoelectron spectroscopy (XPS). The same reactions were done in parallel using silicon wafers and the surface modifications were characterized by ellipsometry.

Immobilization of UCNPs. Excess ligand was removed from PEA-UCNP stock solution using a 100 kDa centrifugal filter. PEA-UCNPs were recovered using a HEPES buffer (100 mM, pH 7.21). Volumes of 2.3 μL of PEA-UCNP solution containing sodium cyanoborohydride in HEPES buffer were spotted on aldehyde coverslips to the desired loading and allowed to incubate as a spot on the surface for the desired amount of time. For the bioassay, 2.3 μL of 10 mg mL^{-1} of UCNP solution was spotted and allowed to incubate for 2 h to ensure uniformity of immobilization. PEA-UCNP and sodium cyanoborohydride solution was also spotted on amine modified coverslips as a control. All surfaces were sonicated in HEPES buffer (100 mM, pH 7.21) for 5 s after incubation. The coverslips were imaged under an epifluorescence microscope setup equipped with a 980 nm laser and a 420−490 nm emission filter. The stability of the immobilized nanoparticles to withstand washing was investigated at three different pH values, 5.5, 7.4, and 8.5. (See Supporting Information.)

Thrombin Detection and Signal Amplification. After UCNP immobilization, 2.3 μL of 1 mM solution of ethanolamine in the presence of sodium cyanoborohydride in the HEPES buffer was spotted and allowed to incubate for 1 h to block aldehyde sites on the coverslip. 2.3 μL of a stock solution made up of 240 μL glutaraldehyde, 360 μL of the HEPES buffer, and 10 mg glutaraldehyde was spotted onto the immobilized UCNPs and left to react for 1 h. This was followed by incubation with 2.3 μL of 3 μM amine modified thrombin-specific aptamer-1 for 6 h. Any remaining aldehyde sites were then blocked using ethanolamine. Thrombin was introduced in AP buffer (50 mM Tris-HCl, 140 mM NaCl, 1 mM $MgCl_2$, 5 mM KCl, pH 7.4)[40] for 6 h followed by 2 μM QD-thrombin-specific aptamer-2 for 6 h. Trilite CdS_xSe_{1-x}/ZnS core/shell QD (614 nm) were purchased from Cytodiagnostics (Burlington, ON, Canada) and QD-aptamer-2 conjugates were prepared based on a literature report in a 5:1 ratio of aptamer-2:QD.[41,42] A detailed procedure and characterization for QD-aptamer-2 conjugates are found in the Supporting Information (Figures S6−S9). Each coverslip was washed three times in reaction buffer after each step. The assay was tested in the presence of BSA and absence of protein as a control. The assay was also performed in 10% (v/v) goat serum. The coverslips were imaged under an epifluorescence microscope setup equipped with a 980 nm laser. A 420−490 nm emission filter was used to collect signals from the UCNPs and 600−640 nm emission filter was used to collect signals from the QDs.

To demonstrate signal enhancement in the case of a closely packed surface, the assay was performed on coverslips where 2, 5, and 10 mg mL^{-1} solutions of UCNPs were spotted, the latter providing for a closely packed surface.

RESULTS AND DISCUSSION

Water-Soluble PEA-UCNPs. PEA-UCNPs were obtained from OA-UCNPs by ligand exchange using PEA. Fourier transform infrared (FTIR) spectroscopy data of OA-UCNPs showed a spectrum that was similar to that of OA. However, the relative intensity of the peak at 1545 cm^{-1} corresponding to the carbonyl stretching frequency of free OA was decreased in the OA-UCNP spectrum. This is consistent with the coordination of the oxygen atoms of the carbonyl functional group to the UCNP surface (Supporting Information Figure S1).[45,46] The exchange of OA with PEA on the surface of the UCNPs was done in excess PEA at an elevated temperature. The use of TMAH allowed for the deprotonation of the phosphates of PEA, promoting ligand exchange with OA. TMAH does not compete for coordination with or degrade the acidic NP surface. Phosphates have been shown to coordinate strongly to UCNP surfaces and are frequently used in ligand exchange reactions to generate water-soluble UCNPs.[37,47,48] Completion of the ligand exchange reaction was confirmed with FTIR spectroscopy by the disappearance of bands associated with OA, and appearance of characteristic PEA peaks (Supporting Information Figure S1). Figure 2a is a TEM

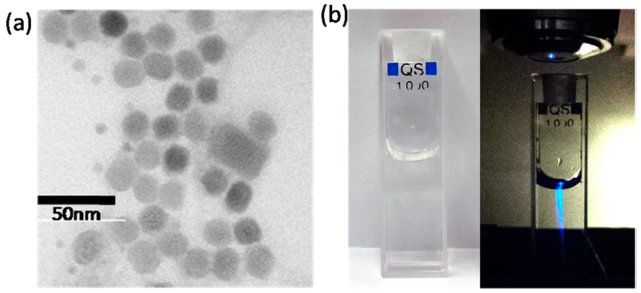

Figure 2. (a) TEM image of PEA-UCNP (b) a clear 16 mg mL^{-1} solution of PEA-UCNP in HEPES buffer (100 mM, pH 7.21) on a white background, and under the objective of a microscope using a 980 nm laser excitation source.

image of PEA-UCNP showing monodisperse UCNPs with an approximate size of 20 nm and the absence of aggregation. This is also supported by DLS data of UCNP size distribution as presented in Supporting Information Figures S2 and S3. Supporting Information Figure S4 shows a positive zeta potential for PEA-UCNP in HEPES buffer (100 mM, pH 7.21) indicating the availability of protonated primary amines on the surface of PEA-UCNPs. Aqueous solutions of PEA-UCNP were obtained with concentrations up to 16 mg mL^{-1} (Figure 2b) and were stable in solution with excess PEA at 4 °C for over 6 months.

Surface Characterization. The surface chemistry on the glass coverslips was characterized using XPS. Results showed high silicon and oxygen content after slides had been cleaned using the RCA protocol. Following reaction with APTMS, a large increase in the carbon and amine content as well as a decrease in the silicon and oxygen content indicated the successful coverage of the glass surface with APTMS (Supporting Information Table S1). Subsequent reaction with glutaraldehyde resulted in a further increase of carbon signal and decrease in silicon signal. The homobifunctional cross-linker glutaraldehyde provided for high density functionalization of aldehyde on the surface, and increased chemical stability by conversion of the primary amines of APTMS into secondary amines.[49] A concentrated solution of glutaraldehyde was used to ameliorate the issue that both of the functional groups of one gluteraldehyde molecule could react with the surface, as demonstrated previously by Park et al.[50]

Silicon wafers that had been processed in parallel to the glass coverslips were evaluated by ellipsometry. Ellipsometry data suggested a relatively uniform surface with an increase of 6.3 ±

0.2 nm after APTMS modification and a further 1.3 ± 0.1 nm after the reaction with glutaraldehyde. The large increase in surface thickness after APTMS modification is consistent with multilayer formation, as has been reported in the literature.[38]

Immobilization Density of Immobilized UCNPs and Signal Amplification. Amine capped UCNPs were immobilized on aldehyde functionalized coverslips via the formation of an imine bond, which was subsequently reduced into a secondary amine using sodium cyanoborohydride. There have been reports of such reactions for other NPs being done in PBS (pH 7.4),[39,49] but in this work, the reaction was performed in HEPES buffer (pH 7.21) because the phosphate salts of the PBS buffer can coordinate to the surface of the UCNPs replacing PEA. The covalently immobilized UCNPs showed stability to washing with buffers of pH 5.5, 7.4, and 8.5 (Supporting Information Figure S12). Control samples were based on PEA-UCNPs that were spotted onto amine functionalized coverslips. The PEA-UCNPs were not retained on the coverslips at any of the various concentrations of UCNPs that were used (Supporting Information Figure S10). This also serves to confirm that primary amines do not coordinate to the surface of the UCNPs to any significant extent, and that PEA coordinates to UCNPs through the phosphate group.

Saturation of the luminescence signal from surfaces covered in the immobilized UCNPs was obtained by treatment using concentrations of about 10 mg mL^{-1} (Supporting Information Figure S11) and subsequent immobilizations made use of this concentration. Saturation of the surface was achieved in less than 30 min (Figure 3). Some reports in the literature about

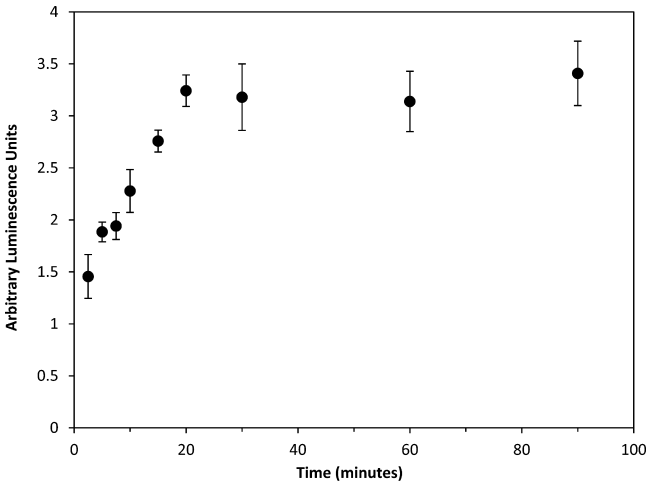

Figure 3. Immobilization from a 10 mg mL^{-1} solution of PEA-UCNPs on aldehyde functionalized coverslips as a function of time. The data was collected using a 420−490 nm band-pass emission filter. Error bars represent 1 standard deviation.

immobilization of other types of NPs have shown similar kinetics. For example, Lau et al.[51] reported that surface saturation by electrostatic adsorption of 79 nm hematite (α-Fe_2O_3) NPs (HNPs) onto bare gold, SAM cysteine modified, and 1-mercapto-11-undecanoic acid modified gold surfaces took less than 30 min. Size-dependent adsorption kinetics were observed, where 79 nm HNPs adsorbed 2−3 times faster than 116 nm HNPs. Given the size of UCNPs (ca. 20 nm) used in our studies, it is reasonable to expect relatively fast immobilization kinetics at high UCNP concentrations.

The ESEM image in Figure 4 shows a closely packed monolayer of UCNPs with a high immobilization density of

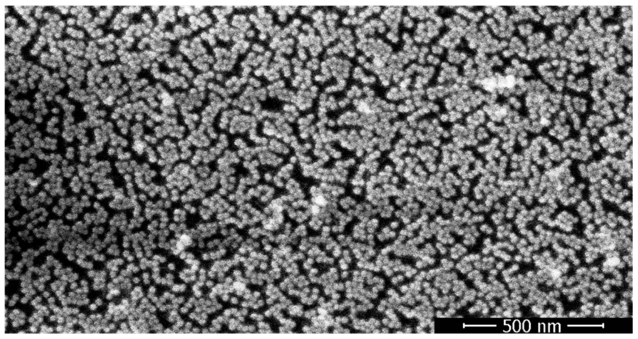

Figure 4. ESEM of immobilized PEA-UCNPs on aldehyde functionalized coverslips.

about 1.3×10^{11} NP cm^{-2} with minimal aggregation. This is consistent with some literature reports on the immobilization of nanoparticles of comparable size. Grabar et al. reported 1.82×10^{11} particles cm^{-2} for 15 nm gold NPs on mercaptopropyltrimethoxysilane coated glass slides,[52] and Petryayeva et al. reported 1.1×10^{11} particles cm^{-2} for 13 nm Au NPs on imidazole surface ligands.[34]

A high surface density is important for the development of solid-phase LRET UCNP-based assay, as the result is increased donor density and improved probability of geometrical arrangements in which a single acceptor can interact with multiple donors. As such, the assay for the detection of thrombin was performed with closely packed UCNPs on the surface (1.3×10^{11} UCNP cm^{-2}) and compared to less densely populated surfaces of approximately 1.0×10^{11} and 7.3×10^{10} UCNP cm^{-2} (Figure 4 and Supporting Information Figure S11). Figure 5 shows that closely packed UCNPs offer a 2.5-fold enhancement in the sensitivity of the LRET ratio between UCNPs and QDs for the detection of thrombin. The close proximity of the UCNPs on the surface increased the donor density and improved the probability of geometrical arrangements in which a single QD acceptor can interact with multiple UCNP donors. Solution and solid-phase LRET studies between UCNPs and QDs were also studied and showed an approximate 1.5-fold enhancement in the LRET ratio for the latter case (Supporting Information Figure S13), giving a potential maximum 3.75-fold overall enhancement. This is consistent with previously reported 4−5-fold enhancements seen on solid-phase Förster resonance energy transfer (FRET) hybridization assays, where hybridization was transduced by Cy3 FRET sensitized emission from immobilized green CdSe/ZnS QD donors.[30]

Thrombin Detection. The closely packed layer of UCNPs was used in an LRET-based bioassay for the detection of thrombin. Aptamer binding to thrombin has been well studied and represents a suitable model for demonstration of a bioassay using UCNPs and LRET. Bednarkiewicz et al. have provided the only report on the physical characteristics of energy transfer to QDs using LRET. Using a dried mixture of Er^{3+} and Yb^{3+} co-doped $NaYF_4$ (ca. 30 nm diameter) and orange CdSe QDs as acceptors, a change in donor emission lifetime from 150 to 130 μs was reported with a Förster distance of only 1.5 nm and an energy transfer efficiency of 14.8%.[53] The energy transfer was thought to occur mostly from Er^{3+} ions close to the surface of the UCNP. For the work reported herein, $NaYF_4$: 0.5% Tm^{3+},

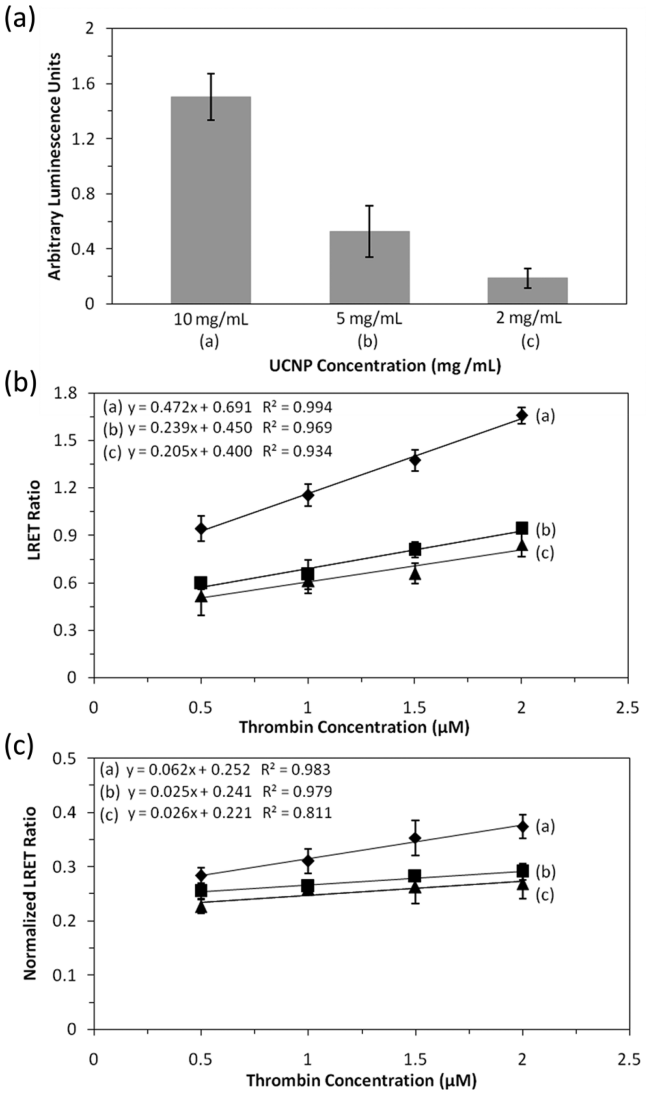

Figure 5. (a) Bar graph showing the concentration of UCNP spotted on the surface giving immobilization densities of 1.3×10^{11}, 1.0×10^{11}, and 7.3×10^{10} UCNP cm^{-2} for 10, 5, and 2 mg mL^{-1} of UCNP solution, respectively. (b) Response curves of LRET ratio between UCNP donors and QD acceptors as a function of thrombin concentration under different UCNP immobilization densities presented in (a). (c) Response curves of LRET ratio from (b) normalized to the number of QD acceptors present. The results for UCNP luminescence and QD luminescence were collected using 420−490 nm and 600−640 nm emission filters, respectively. Error bars represent 1 standard deviation.

30% $Yb^{3+}/NaYF_4$ core/shell UCNPs and CdS_xSe_{1-x}/ZnS core/shell 614 nm QDs were used as the donor−acceptor system, as depicted in Figure 1. Figure 6 shows the spectral overlap between the UCNP emission and QD absorption, where both pairs of the emission peaks (in the UV and blue-green region of the spectrum) of the UCNPs can contribute to LRET. Since the UCNPs did not exhibit emission near 614 nm, QD emission was collected with little optical background.

It is important to note that even though the Er^{3+}/Yb^{3+} couple exhibits more efficient UC compared to the Tm^{3+}/Yb^{3+} couple used herein, the latter offers greater spectral overlap between the UV and purple emission peaks of the UCNP and the absorption spectrum of the QD, allowing for efficient LRET. In addition, Er^{3+}/Yb^{3+} couples can exhibit a strong emission peak

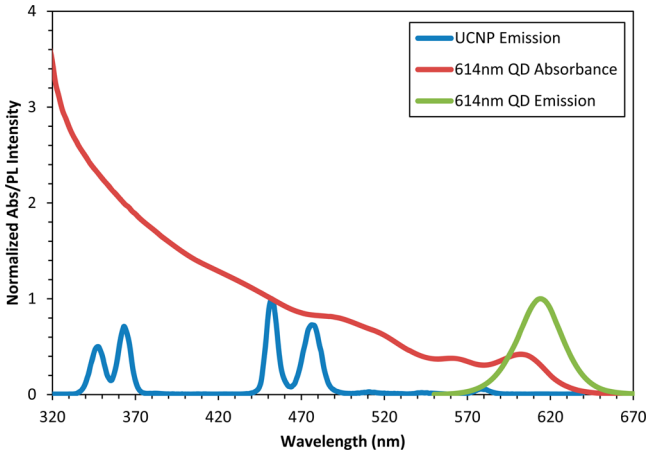

Figure 6. Overlay of $NaYF_4$: 0.5% Tm^{3+}, 30% Yb^{3+}/β-$NaYF_4$ core/shell UCNP emission spectrum (excitation 980 nm, ca. 500 mW mm^{-2}) and red QD absorption and emission spectra (excitation 405 nm).

in the red region, which overlaps with that of the QDs and increases background signal in the acceptor channel.

A linear correlation between the amount of thrombin and the LRET ratio for the sandwich based assay in buffer and 10% (v/v) goat serum is shown in Figure 7 with negligible background

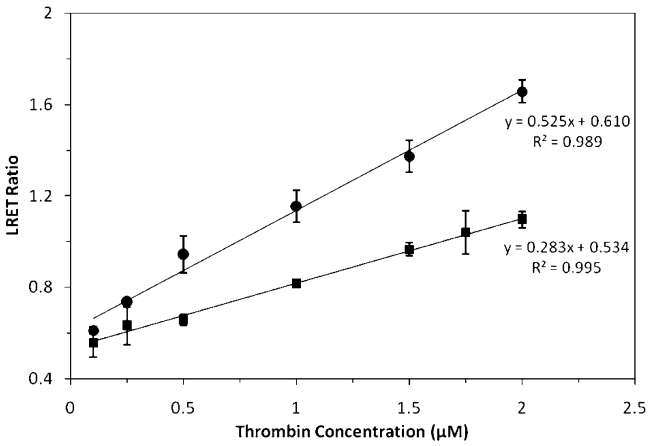

Figure 7. Calibration curve showing the change in LRET ratio between UCNP donors and QD acceptors as a function of thrombin concentration ranging from 0.1 μM to 2 μM in buffer (circle) and 10% (v/v) goat serum (square). Error bars represent 1 standard deviation.

signal from the near IR excitation source (Supporting Information Figure S14). In both cases, a limit of detection of 230 fmol using a 2.3 μL sample volume (0.1 μM) was experimentally determined, lower than the normal thrombin concentration found in human blood, which is about 1.3 μM.[54] The selectivity of the aptamers to thrombin makes it feasible to use the assay in a complex matrix. The selectivity of the assay was tested against BSA, showing an 80% lower signal for 1 μM BSA compared to 0.1 μM thrombin (Figure 8). The nonspecific adsorption of QDs onto the surface was examined in the absence of any protein and showed minimal nonspecific adsorption with a signal that was 90% lower compared to 0.1 μM thrombin (Figure 8). A similar solution-phase assay for the detection of thrombin using UCNPs as donors and gold nanorods as acceptors has been reported in the literature.[55] A limit of detection of 3.25 nM in a 100-fold diluted serum

dx.doi.org/10.1021/am503391m | ACS Appl. Mater. Interfaces 2014, 6, 14061−14068

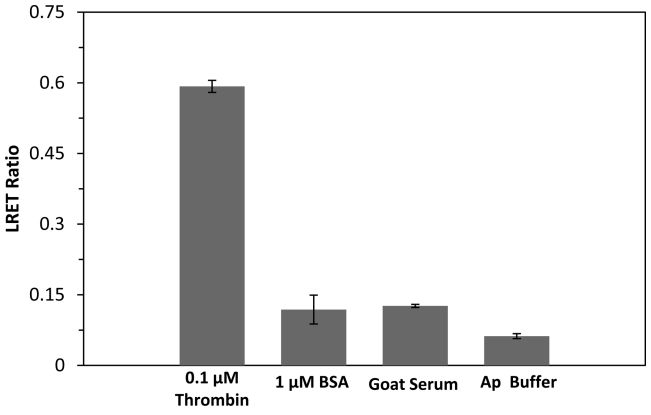

Figure 8. Assay response from 0.1 μM thrombin, 1 μM BSA, and absence of protein in 10% (v/v) goat serum and AP Buffer. The BSA and goat serum samples demonstrate the selectivity of the assay and the absence of any proteins in AP Buffer demonstrates minimal nonspecific adsorption of QD-Aptamer 2 conjugates on the surface. Error bars represent 1 standard deviation.

sample was reported. However, details about sample specifications are unavailable to complete a quantitative comparison of assay performance. Nonetheless, the performance of our assay in buffer and serum successfully demonstrated the physical stability of immobilized UCNPs on the surface.

CONCLUSION

We have demonstrated the covalent immobilization of UCNPs on glass substrate. A uniform monolayer of closely packed amine capped UCNPs was obtained on aldehyde functionalized coverslips with an immobilization density of ca. 1.3×10^{11} NP cm^{-2}. The stability of the UCNPs on the surface allowed for their use as donors in an LRET based assay for the detection of thrombin using two thrombin specific aptamers and red emitting QDs as acceptors. The use of UCNPs as donors at an interface demonstrated better LRET ratio compared to solution-phase studies. Glass surface with closely packed UCNPs exhibited 2.5-fold improved sensitivity in the detection of thrombin over less densely packed surfaces. Compared to the inherent background signal associated with the use of UV radiation for direct excitation of QDs, the use of a near-IR laser for excitation of UCNPs suppressed the background signal by 8-fold. Overall, this work indicates a facile strategy for the covalent immobilization of UCNPs on solid supports and we expect such schemes will help develop LRET-based solid-phase bioassays for UCNPs.

ASSOCIATED CONTENT

Supporting Information

Experimental techniques, instrumentation, UCNP characterization and stability, solid-phase signal enhancement, and additional results. This material is available free of charge via the Internet at http://pubs.acs.org.

AUTHOR INFORMATION

Corresponding Author

*E-mail: ulrich.krull@utoronto.ca.

Author Contributions

Samer Doughan and Yi Han contributed equally to this work.

Notes

The authors declare no competing financial interest.

ACKNOWLEDGMENTS

We thank Dr. Sreekumari Nair for obtaining TEM images, Dr. Neil Coombs and Dr. Ilya Gourevich for help with ESEM, and Dr. Rana Sodhi for obtaining XPS results. We gratefully acknowledge the Natural Sciences and Engineering Research Council of Canada (NSERC) for financial support of this research. S.D. and U.U. are also grateful to NSERC for graduate fellowships.

REFERENCES

(1) Zhou, J.; Liu, Z.; Li, F. Upconversion Nanophosphors for Small-Animal Imaging. *Chem. Soc. Rev.* **2012**, *41*, 1323−1349.
(2) Wang, F.; Banerjee, D.; Liu, Y. S.; Chen, X. Y.; Liu, X. G. Upconversion Nanoparticles in Biological Labeling, Imaging, and Therapy. *Analyst* **2010**, *135*, 1839−1854.
(3) DaCosta, M. V.; Doughan, S.; Han, Y.; Krull, U. J. Lanthanide Upconversion Nanoparticle and Applications in Bioassays and Bioimaging: A Review. *Anal. Chim. Acta* **2014**, *832*, 1−33.
(4) Auzel, F. Upconversion and Anti-Stokes Processes with f and d Ions in Solids. *Chem. Rev.* **2003**, *104*, 139−174.
(5) Cheng, L. A.; Yang, K.; Zhang, S. A.; Shao, M. W.; Lee, S. T.; Liu, Z. A. Highly-Sensitive Multiplexed in vivo Imaging Using PEGylated Upconversion Nanoparticles. *Nano Res.* **2010**, *3*, 722−732.
(6) Dou, Q.; Idris, N. M.; Y, Z. Sandwich-Structured Upconversion Nanoparticles with Tunable Color for Multiplexed Cell Labeling. *Biomaterials* **2013**, *34*, 1722−1731.
(7) Zijlmans, H. J. M. A. A.; Bonnet, J.; Burton, J.; Kardos, K.; Vail, T.; Niedbala, R. S.; Tanke, H. J. Detection of Cell and Tissue Surface Antigens Using Up-Converting Phosphors: A New Reporter Technology. *Anal. Biochem.* **1999**, *267*, 30−36.
(8) Niedbala, R. S.; Feindt, H.; Kardos, K.; Vail, T.; Burton, J.; Bielska, B.; Li, S.; Milunic, D.; Bourdelle, P.; Vallejo, R. Detection of Analytes by Immunoassay Using Up-Converting Phosphor Technology. *Anal. Biochem.* **2001**, *293*, 22−30.
(9) Hampl, J.; Hall, M.; Mufti, N.; Yao, Y. M.; MacQueen, D. B.; Wright, W. H.; Cooper, D. E. Upconverting Phosphor Reporters in Immunochromatographic Assays. *Anal. Biochem.* **2001**, *288*, 176−187.
(10) Corstjens, P. L. A. M.; van Lieshout, L.; Zuiderwijk, M.; Kornelis, D.; Tanke, H. J.; Deelder, A. M.; van Dam, G. J. Up-Converting Phosphor Technology-Based Lateral Flow Assay for Detection of *Schistosoma* Circulating Anodic Antigen in Serum. *J. Clin. Microbiol.* **2008**, *46*, 171−176.
(11) Corstjens, P. L. A. M.; Zuiderwijk, M.; Tanke, H. J.; van der Ploeg-van Schip, J. J.; Ottenhoff, T. H. M.; Geluk, A. A User-Friendly, Highly Sensitive Assay to Detect the IFN-γ Secretion by T cells. *Clin. Biochem.* **2008**, *41*, 440−444.
(12) Kuningas, K.; Rantanen, T.; Ukonaho, T.; Lövgren, T.; Soukka, T. Homogeneous Assay Technology Based on Upconverting Phosphors. *Anal. Chem.* **2005**, *77*, 7348−7355.
(13) Yuan, Y.; Liu, Z. An Effective Approach to Enhanced Energy-Transfer Efficieny from Up-Converting Phosphors and Increased Assay Sensitivity. *Chem. Commun.* **2012**, *48*, 7510−7512.
(14) Lin, F.; Yin, B.; Ii, C.; Deng, J.; Fan, X.; Yi, Y.; Liu, C.; Li, H.; Zhang, Y.; Yao, S. Fluorescence Resonance Energy Transfer Aptasensor for Platelet-Derived Growth Factor Detection Based on Upconversion Nanoparticles in 30% Blood Serum. *Anal. Methods* **2013**, *5*, 699−704.
(15) Wang, Y.; Bao, L.; Liu, Z.; Pang, D. Aptamer Biosensor Based on Fluorescence Resonance Energy Transfer from Upconverting Phosphors to Carbon Nanoparticles for Thrombin Detection in Human Plasma. *Anal. Chem.* **2011**, *83*, 8130−8137.
(16) Wang, Y.; Shen, P.; Li, C.; Wang, Y.; Liu, Z. Upconversion Fluorescence Resonance Energy Transfer Based Biosensor for Ultrasensitive Detection of Matrix Metalloproteinase-2 in Blood. *Anal. Chem.* **2012**, *84*, 1466−1473.
(17) Corstjens, P. L. A. M.; Zuiderwijk, M.; Nilsson, M.; Feindt, H.; Niedbala, R. S.; Tanke, H. J. Lateral-Flow and Up-Converting

Phosphor Reporters to Detect Single-Stranded Nucleic Acids in a Sandwich-Hybridization Assay. *Anal. Biochem.* **2003**, *312*, 191−200.
(18) Zuiderwijk, M.; Tanke, H. J.; Niedbala, R. S.; Corstjens, P. An Amplification-Free Hybridization-Based DNA Assay to Detect *Streptococcus Pneumoniae* Utilizing the Up-Converting Phosphor Technology. *Clin. Biochem.* **2003**, *36*, 401−403.
(19) Kumar, M.; Guo, Y.; Zhang, P. Highly Sensitive and Selective Oligonucleotide Sensor for Sickle Cell Disease Gene Using Photon Upconverting Nanoparticles. *Biosens. Bioelectron.* **2009**, *24*, 1522−1526.
(20) Rantanen, T.; Järvenpää, M.; Vuojola, J.; Arppe, R.; Kuningas, K.; Soukka, T. Upconverting Phosphors in a Dual-Parameter LRET-Based Hybridization Assay. *Analyst* **2009**, *134*, 1713−1716.
(21) Wu, S.; Duan, N.; Wang, Z.; Wang, H. Aptamer-Functionalized Magnetic Nanoparticles-Based Bioassay for the Detection of Ochratoxin a Using Upconversion Nanoparticles as Labels. *Analyst* **2011**, *136*, 2306−2314.
(22) Kuningas, K.; Ukonaho, T.; Päkkilä, H.; Rantanen, T.; Rosenberg, J.; Lövgren, T.; Soukka, T. Upconversion Fluorescence Resonance Energy Transfer in a Homogeneous Immunoassay for Estradiol. *Anal. Chem.* **2006**, *78*, 4690−4696.
(23) Kannan, P.; Abdul Rahim, F.; Chen, R.; Teng, X.; Huang, L.; Sun, H.; Kim, D. Au Nanorod Decoration on $NaYF_4$:Yb/Tm Nanoparticles for Enhanced Emission and Wavelength-Dependent Biomolecular Sensing. *ACS Appl. Mater. Interfaces* **2013**, *5*, 3508−3513.
(24) Kumar, M.; Zhang, P. Highly Sensitive and Selective Label-Free Optical Detection of Mercuric Ions Using Photon Upconverting Nanoparticles. *Biosens. Bioelectron.* **2010**, *25*, 2431−2435.
(25) Liu, B.; Tan, H.; Chen, Y. Upconversion Nanoparticles-Based Fluorescence Energy Transfer Assay for Cr(III) Ions in Urine. *Anal. Chim. Acta* **2013**, *761*, 178−185.
(26) Guo, H. C.; Hao, R. Z.; Qian, H. S.; Sun, S. Q.; Sun, D. H.; Yin, H.; Liu, Z. X.; Liu, X. T. Upconversion Nanoparticles Modified with Aminosilanes as Carriers of DNA Vaccine for Foot-and-Mouth Disease. *Appl. Microbiol. Biotechnol.* **2012**, *95*, 1253−1263.
(27) Li, H.; Wang, L. $NaYF_4$:Yb^{3+}/Er^{3+} Nanoparticle-Based Upconversion Luminescence Resonance Energy Transfer Sensor for Mercury(II) Quantification. *Analyst* **2013**, *138*, 1589−1595.
(28) He, M.; Liu, Z. Paper-Based Microfluidic Device with Upconversion Fluorescence Assay. *Anal. Chem.* **2013**, *85*, 11691−11694.
(29) Zhou, F.; Noor, M. O.; Krull, U. J. Luminescence Resonance Energy Transfer-Based Nucleic Acid Hybridization Assay on Cellulose Paper with Upconverting Phosphor as Donors. *Anal. Chem.* **2014**, *86*, 2719−2726.
(30) Tavares, A. J.; Noor, M. O.; Vannoy, C. H.; Algar, W. R.; Krull, U. J. On-Chip Transduction of Nucleic Acid Hybridization Using Spatial Profiles of Immobilized Quantum Dots and Fluorescence Resonance Energy Transfer. *Anal. Chem.* **2012**, *84*, 312−319.
(31) Petryayeva, E.; Algar, W. R.; Krull, U. J. Adapting Fluorescence Resonance Energy Transfer with Quantum Dot Donors for Solid-Phase Hybridization Assays in Microtiter Plate Format. *Langmuir* **2013**, *29*, 977−987.
(32) Noor, M. O.; Petryayeva, E.; Tavares, A. J.; Uddayasankar, U.; Algar, W. R.; Krull, U. J. Building from the "Ground" Up: Developing Interfacial Chemistry for Solid-Phase Nucleic Acid Hybridization Assays Based on Quantum Dots and Fluorescence Resonance Energy Transfer. *Coord. Chem. Rev.* **2014**, *263*−*264*, 25−52.
(33) Kumar, M.; Zhang, P. Highly Sensitive and Selective Label-Free Optical Detection of DNA Hybridization Based on Photon Upconverting Nanoparticles. *Langmuir* **2009**, *25*, 6024−6027.
(34) Petryayeva, E.; Krull, U. J. Quantum Dot and Gold Nanoparticle Immobilization for Biosensing Applications using Multidentate Imidazole Surface Ligands. *Langmuir* **2012**, *28*, 13943−13951.
(35) Nath, N.; Chilkoti, A. A Colorimetric Gold Nanoparticle Sensor to Interrogate Biomolecular Interactions in Real Time on a Surface. *Anal. Chem.* **2002**, *74*, 504−509.
(36) Carling, C. J.; Nourmohammadian, F.; Boyer, J. C.; Branda, N. R. Remote-Control Photorelease of Caged Compounds Using Near-Infrared Light and Upconverting Nanoparticles. *Angew. Chem., Int. Ed.* **2010**, *49*, 3782−3785.
(37) Boyer, J. C.; Manseau, M. P.; Murray, J. I.; Van Veggel, F. C. J. M. Surface Modification of Upconverting $NaYF_4$ Nanoparticles with PEG-Phosphate Ligands for NIR (800 nm) Biolabeling within the Biological Window. *Langmuir* **2010**, *26*, 1157−1164.
(38) Algar, W. R.; Krull, U. J. Multidentate surface ligand exchange for the immobilization of CdSe/ZnS quantum dots and surface quantum dot-oligonucleotide conjugates. *Langmuir* **2008**, *24*, 5514−5520.
(39) Noor, M. O.; Krull, U. J. Microfluidics for the Deposition of Density Gradients of Immobilized Oligonucleotide Probes; Developing Surfaces That Offer Spatial Control of the Stringency of DNA Hybridization. *Anal. Chim. Acta* **2011**, *708*, 1−10.
(40) Tennico, Y. H.; Hutanu, D.; Koesdjojo, M. T.; Bartel, C. M.; Remcho, V. T. On-Chip Aptamer-Based Sandwich Assay for Thrombin Detection Employing Magnetic Beads and Quantum Dots. *Anal. Chem.* **2010**, *82*, 5591−5597.
(41) Noor, M. O.; Krull, U. J. Paper-Based Solid-Phase Multiplexed Nucleic Acid Hybridization Assay with Tunable Dynamic Range Using Immobilized Quantum Dots as Donors in Fluorescence Resonance Energy Transfer. *Anal. Chem.* **2013**, *85*, 7502−7511.
(42) Noor, M. O.; Shahmuradyan, A.; Krull, U. J. Paper-Based Solid-Phase Nucleic Acid Hybridization Assay Using Immobilized Quantum Dots as Donors in Fluorescence Resonance Energy Transfer. *Anal. Chem.* **2013**, *85*, 1860−1867.
(43) Tasset, D. M.; Kubik, M. F.; Steiner, W. Oligonucleotide Inhibitors of Human Thrombin That Bind Distinct Epitopes. *J. Mol. Biol.* **1997**, *272*, 688−698.
(44) Bock, L. C.; Griffin, L. C.; Latham, J. A.; Vermaas, E. H.; Toole, J. J. Selection of Single-Stranded DNA Molecules That Bind and Inhibit Human Thrombin. *Nature* **1992**, *355*, 564−566.
(45) Sarkar, S.; Hazra, C.; Mahalingam, V. Scaling Down the Size of $BaLnF_5$ Nanocrystals (Ln = La, Gd, and Lu) with the Ln^{3+} Size. *Dalton Trans.* **2013**, *42*, 63−66.
(46) Zhang, L.; He, R.; Gu, H. C. Oleic Acid Coating on the Monodisperse Magnetite Nanoparticles. *Appl. Surf. Sci.* **2006**, *253*, 2611−2617.
(47) Diamente, P. R.; Van Veggel, F. C. J. M. Water-Soluble Ln^{3+}-Doped LaF_3 Nanoparticles: Retention of Strong Luminescence and Potential as Biolabels. *J. Fluoresc.* **2005**, *15*, 543−551.
(48) Wu, T.; Barker, M.; Arafeh, K. M.; Boyer, J. C.; Carling, C. J.; Branda, N. R. A UV-Blocking Polymer Shell Prevents One-Photon Photoreactions While Allowing Multi-Photon Processes in Encapsulated Upconverting Nanoparticles. *Angew. Chem., Int. Ed.* **2013**, *52*, 11106−11109.
(49) Goddard, J. M.; Erickson, D. Bioconjugation Techniques for Microfluidic Biosensors. *Anal. Bioanal. Chem.* **2009**, *394*, 469−479.
(50) Park, S. H.; Krull, U. A Spatially Resolved Nucleic Acid Biochip Based on a Gradient of Density of Immobilized Probe Oligonucleotide. *Anal. Chim. Acta* **2006**, *564*, 133−140.
(51) Lau, B. L. T.; Huang, R.; Madden, A. S. Electrostatic Adsorption of Hematite Nanoparticles on Self-Assembled Monolayer Surfaces. *J. Nanopart. Res.* **2013**, *15*, 1873.
(52) Grabar, K. C.; Smith, P. C.; Musick, M. D.; Davis, J. A.; Walter, D. G.; Jackson, M. A.; Guthrie, A. P.; Natan, M. J. Kinetic Control of Interparticle Spacing in Au Colloid-Based Surfaces: Rational Nanometer-Scale Architecture. *J. Am. Chem. Soc.* **1996**, *118*, 1148−1153.
(53) Bednarkiewicz, A.; Nyk, M.; Samoc, M.; Strek, W. Up-Conversion FRET From Er^{3+}/Yb^{3+}:$NaYF_4$ Nanophosphor to CdSe Quantum Dots. *J. Phys. Chem. C* **2010**, *114*, 17535−17541.
(54) Putman, F. W. *The Plasma Proteins: Structure, Function, and Genetic Control*; Academic Press Inc.: United States of America, 1960; Vol. *2*.
(55) Chen, H.; Yuan, F.; Wang, S.; Xu, J.; Zhang, Y.; Wang, L. Aptamer-Based Sensing for Thrombin in Red Region via Fluorescence Resonant Energy Transfer Between $NaYF_4$:Yb,Er Upconversion

Nanoparticles and Gold Nanorods. *Biosens. Bioelectron.* **2013**, *48*, 19−25.